IAC-18,C4,10,2,x47422

LOX-METHANE COMBUSTION CHARACTERISTICS IN SWIRL COAXIAL INJECTOR OF LOX- HYDROGEN ENGINE

Abhishek Sharma[a*], Arjun C K[b], S.Sunil Kumar[a], Gireesh Kumaran Thampi[b]

[a]*Liquid Propulsion Systems Centre, Indian Space Research Organisation*
Thiruvananthapuram, Kerala-695547, India,
[b]*Cochin University of Science and Technology, Kerala-682 022 India*
abhisheksharma@lpsc.gov.in
*Corresponding Author

Abstract

Propellant combinations such as Liquid Oxygen (LOx)-hydrogen and LOx-kerosene are commonly used in liquid rocket engines. Recently, LOx-methane combination has attracted considerable attention for future development of reusable launch vehicles (RLV). Methane is widely accepted as an alternative fuel for new generation propulsion systems because of soft cryogenic, high density impulse and low coking properties. A possibility of converting existing LOx-hydrogen rocket propulsion system to LOx-methane is under consideration among space agencies. It is essential to understand the combustion characteristics/efficiency of methane for any possible conversion of existing hydrogen propelled rocket engine. In regard to same, a numerical study is initiated to explore and compare combustion characteristics of LOx-methane in a swirl coaxial injector of existing hydrogen propulsion system. A Computational Fluid Dynamics (CFD) model is developed to study combustion characteristics at supercritical pressure of 6.8MPa. In this study, LOx is injected through 4 tangential inlets and gaseous methane/hydrogen is injected axially through a swirled path. The non-ideal thermo-physical properties are modelled using Soave-Redlich-Kwong (SRK) real gas equation of state and chemistry closure is achieved using non-premixed probability density function (PDF) based chemical equilibrium approach. Favre-averaged Navier-stokes equations are solved using finite volume methodology with SST k-ω model for turbulence closure. A validated methodology is developed based on Mascotte chamber RCM-3 (V04) test. Numerical results showed good agreement with literature result from Kim et al. RCM-3 (V04) test case. A detailed comparison of hydrogen and methane flame shape in single element domain is carried out. Results showed localized difference in flame shape/structures in methane and hydrogen combustion cases. A larger and rapid radial expansion of flame was seen for hydrogen compared to LOx-methane case. Both simulations showed, flame anchored at fuel post and formation of recirculation region to help in flame stabilization by further igniting the incoming propellants.

Keywords: rocket; combustion; methane; oxygen; Mascotte

$\bar{}$	= averaged quantity
~	= favre averaged quantity
P	= pressure
R	= universal gas constant
T	= temperature
V	= molar volume
a	= coefficient to account for attraction
b	= coefficient to account for repulsion
ω	= acentric factor
T_c	= critical temperature
P_c	= critical pressure
e	= entropy
h	= enthalpy
C_p	= constant pressure specific heat
u	= velocity
μ	= molecular viscosity
μ_t	= turbulent viscosity
k	= turbulent kinetic energy
ε	= turbulent dissipation energy
ν	= kinematic viscosity
Z	= mixture fraction
μ_{eff}	= effective diffusivity

1. Introduction

In recent years, reusable launch vehicle (RLV) has been the focus of research in space applications. Liquid Rocket Engine (LRE) is regarded as best option for the propulsion system of RLV because of the high thrust, high reliability, and low cost. Compared to other fuel propellants, liquid hydrogen (LH_2) holds the advantage of having high specific impulse and better combustion properties, when mixed with Liquid Oxygen (LOx). However, the low density of LH_2 leads to a larger tank volume, heavier vehicle mass, and higher aerodynamic drag. These drawbacks paved the way for hydrocarbons with better combustion and cryogenic properties which are very much economic compared to hydrogen. Kerosene is the widely used hydrocarbon rocket propellant because of its advantages over LH_2, but methane because of its lower viscosity and higher specific heat capacity compared to kerosene, can provide better combustion characteristics. Methane has a storage temperature similar to Liquid Oxygen, which makes the design properties of the tank simple compared to hydrogen storage systems. In addition, methane has the highest specific impulse among hydrocarbon fuels and, it has better metal compatibility due to its sooting, coking and corrosion characteristics.

Most of Lox-Hydrogen propulsion systems employ swirl injectors to achieve efficient mixing and combustion. The swirling motion of propellants primarily improve the flame stability Generally swirl injectors are broadly divided into two types, gas centred swirl coaxial injector (GCSC) and liquid centred swirl coaxial injector (LCSC). The difference lies in the swirling of liquid in the injector. Atomization is achieved by the breakup of the swirling liquid sheet. The breakup process includes thinning and perforation of liquid sheet, ligaments and droplets.

Combustion process in rocket engine solely relies on the pressure and temperature parameters of the injected propellants. The thrust requirement in these engines demands supercritical conditions inside the combustion chamber. Under supercritical conditions, the behaviour of the injected propellants shows large variations. The thermodynamic properties are largely influenced by these conditions, and shows different characteristics compared to that at subcritical conditions. Behaviour of a pure substance at different pressure and temperature conditions is shown as a phase diagram which is depicted in Figure1. On approaching the critical point, surface tension tends to decrease and there will be no clear phase separating the fluids. As a result, it shows both liquid and gaseous behaviour, which includes liquid like density and gas like diffusivity. At supercritical conditions, the aerodynamic force diminishes and jet experiences a variable density gas like mixing process, with large variation in thermodynamic properties. In most of the rocket engines, the injection conditions of one or both propellants is above the critical point. Liquid Oxygen is introduced in most of the cases in transcritical conditions and the other propellant in supercritical condition. Under transcritical conditions, propellants show large changes in behaviour which is produced by the pseudo-boiling phenomenon. Numerical modelling of such high pressure conditions poses a complex challenge in analysing the characteristics of the propellants.

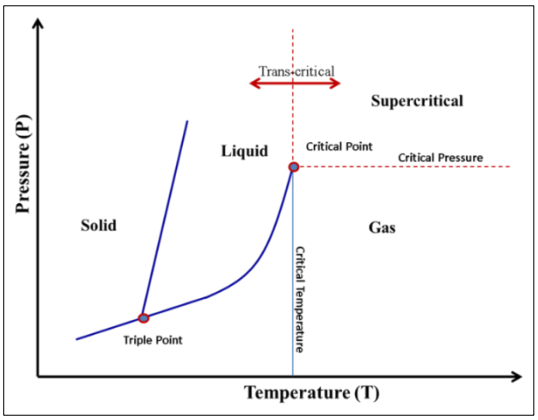

Figure 1 Phase diagram for any pure substance

A number of studies have been carried out on supercritical combustion of LOx/methane and LOx/hydrogen combination in both shear and swirl coaxial injectors. Recent developments are solely focussed on swirl coaxial injectors mainly due to its efficient mixing and atomization properties. Mayer *et al.* [1] discussed about the importance of real gas effects on the modelling of combustion characteristics of propellants at supercritical and transcritical conditions. It showed the role of chamber pressure in the formation and mixing of smaller droplets and ligaments, which further affects the atomization process. Study showed that, with increase in chamber pressure, capillary forces diminishes and gas like mixing causes the atomization. Congiunti *et al* [2] compared various equation of states considering the importance of real gas modelling of propellants under supercritical conditions. He compared various cubic equation of states and concluded that Soave-Redlich-Kwong (SRK) equation of state is the best option for real gas modelling at all conditions, except at critical zone, where Peng-Robinson (PR) equation of state is accurate. Emre Sozer *et al* [3] did simulation of GO_2/GH_2 flame with laminar finite rate combustion model (LFR) and chemical equilibrium and chemical non-equilibrium models with non-premixed assumed probability density function

(PDF). SST k-ω model was used for turbulence-closure. Results showed similarity in both chemical equilibrium and chemical non-equilibrium formulation, which was attributed to non-existent non-equilibrium effects in GO_2/GH_2 chemistry. It highlighted that LFR model predicted higher temperature near stoichiometric flame surface compared to non-premixed combustion model. Study compared experimental wall heat flux with simulation for near wall region and in recirculating region. Strakey *et al* [4] worked on mixing characteristics of coaxial injectors at high gas/liquid momentum ratios. He did experiment on LOx/LH_2 at two chamber pressures of 2.96MPa and 10.3 MPa, and compared results with SSME pre burner injector tests. Study showed that, with increase in gas/liquid momentum ratio, spray cone angle decreased. Liang Li *et al.* [5] did numerical modelling at both supercritical and transcritical conditions and explained the difference in characteristics of jets injected at both conditions. Study highlighted effects of pseudo-boiling phenomenon on combustion characteristics of propellants injected at transcritical conditions. The mixing layer was observed to be very thin, as all the energy available was utilized for expanding the volume. In contrast, for supercritical jets, thick mixing layer had formed, where energy available was used for temperature rise rather than volume expansion. Shingo Matsuyama *et al* [6] did Large Eddy Simulation of CH_4/O_2 combustion of a swirl coaxial injector. He analysed two different flame structures (attached and lifted flames) by varying the location of heat source for igniting the propellant mixture. Ata Poormahmood *et al.* [7] studied about the recirculation zone downstream of swirl coaxial injector. Their study also showed flame to get stabilized by a central toroidal recirculation zone (CTRZ). This CTRZ is accompanied by a central vortex core (CVC) and precessing vortex core (PVC) which further affects the spray cone angle of the liquid sheet. PVC structures were seen to be compressed with increase in ambient pressure, thereby reducing the effects of instabilities. Takao Inamura *et al*. [8] explained the spray characteristics of propellants at subcritical and supercritical conditions. His study showed that, at subcritical conditions surface tension predominates, and there will be clear phase distinction within fluids. A thread like structures were seen to form in supercritical conditions which can be regarded as fluid-fluid mixing. Baoe Yang *et al* [9] did experimental work on atomization and flames in CH_4/LOx spray combustion. His work was mainly focussed on analysing the influence of fuel properties and its kinetics on atomization and LOx/CH_4 and LOx/H_2 spray combustion. Injection conditions with varying Weber number and momentum flux ratio were done and the results showed that LOx/CH_4 sprays exhibit shorter liquid oxygen core length compared to LOx/LH_2 at similar Weber number and momentum flux ratio. Also, it was found that the momentum flux ratio determines the primary breakup and corresponding core length while, the Weber number influences the secondary atomization and flame length. Dalphin Salgues *et al* [10] worked on shear and swirl coaxial injector studies of LOx/GCH_4 combustion using non-intrusive laser diagnostics. He compared different configuration of injectors operating on methane. Light scattering, shadowgraph imaging techniques and OH-PLIF were used for visualization and comparison among injectors. Study showed that the radial expansion of flame in shear coaxial injector is smaller compared to swirl coaxial injectors. Study concluded that swirl injectors provide highest gas velocity and rapid atomization and mixing compared to shear coaxial injector. Vigor Yang *et al* [11] analysed supercritical mixing and combustion of LOx/kerosene on bi-swirl injectors with LES model and turbulence/chemistry interaction using laminar flamelet library approach. Study concluded that strong swirling motion and corresponding centrifugal forces produced larger pressure gradient in the radial direction leading to development of LOx film along the injector wall, whereas recess region resulted in larger spreading angle in the LOx region. Study with reacting flow dynamics showed counter rotating recirculation zone in the wake region, which seen to help in stabilizing and preheating the fresh propellants.

In spite of many numerical studied conducted separately on LOx/methane and LOx/hydrogen combination in swirl injector at supercritical conditions. A comparative study has not been done to assess the flow and flame characteristics of LOx-Methane combination operating in swirl injector of hydrogen propulsion system. Present work is focussed on studying the combustion characteristics of LOx/methane to evaluate the possibility of converting existing LOx/hydrogen rocket propulsion system to LOx/methane.

The paper presents a detailed comparison of flow and combustion characteristics of LOx/methane and LOx/hydrogen propellant combination at single element level. Due to highly complex flow physics associated with swirl coaxial injectors, comparative study for both propellant combination is done at single injector element level only. The paper presents cold flow comparison followed by comparative analysis on combustion modelling for both hydrogen and methane cases. The paper finally reports major difference in flow and flame fields for Lox-methane combination operating in injector of Lox-hydrogen propulsion system.

2. Numerical methodology

2.1. Favre Averaged Governing Equations

Density fluctuations play a major role in turbulent combustion modelling. Density weighted average of each variable is taken into consideration which is called Favre averaging. The theoretical formulation is based on Favre averaged mass continuity, momentum, energy and species conservation equations. The governing equations can be written as:

$$\frac{\partial \tilde{\rho}}{\partial t} + \frac{\partial \bar{\rho}\tilde{u}_j}{\partial x_j} = 0 \quad (1)$$

$$\frac{\partial \bar{\rho}\tilde{u}_i}{\partial t} + \frac{\bar{\rho}\tilde{u}_j\tilde{u}_i}{\partial x_j} = -\frac{\partial \bar{\rho}}{\partial x_i} + \frac{\partial}{\partial x_j}\left(\tilde{\tau}_{ij} - \overline{\rho u_i'' u_j''}\right) \quad (2)$$

The shear stress term for a Newtonian fluid is written as:

$$\tilde{\tau}_{ij} = \mu\left(\frac{\partial \tilde{u}_i}{\partial x_j} + \frac{\partial \tilde{u}_j}{\partial x_i}\right) - \frac{2}{3}\mu\frac{\partial \tilde{u}_k}{\partial x_k}\delta_{ij}$$

Where fluctuations in the dynamic viscosity term are neglected. Also $\overline{\rho u_i'' u_j''}$ is a Reynolds stress term given by;

$$-\overline{\rho u_i'' u_j''} = \mu_t\left(\frac{\partial \tilde{u}_i}{\partial x_j} + \frac{\partial \tilde{u}_j}{\partial x_i}\right) - \frac{2}{3}\mu_t\frac{\partial \tilde{u}_k}{\partial x_k}\delta_{ij} - \frac{2}{3}\bar{\rho}k\delta_{ij}$$

$$\frac{\partial}{\partial t}\left(\bar{\rho}\widetilde{H} - \bar{p}\right) + \frac{\partial}{\partial x_j}\left(\bar{\rho}\tilde{u}_j\widetilde{H}\right) = \frac{\partial}{\partial x_j}\left[\left(\frac{\mu}{Pr} + \frac{\mu_t}{Pr_t}\right)\frac{\partial \tilde{h}}{\partial x_j}\right] + \frac{\partial}{\partial x_j}\left[\tilde{u}_j(\mu + \mu_t)\left(\frac{\tilde{u}_i}{x_j} + \frac{\tilde{u}_j}{x_i} - \frac{2}{3}\frac{\partial \tilde{u}_k}{\partial x_k}\delta_{ij}\right)\right] + \frac{\partial}{\partial x_j}\left[(\mu + \mu_t\sigma_k)\frac{\partial k}{\partial x_j}\right] \quad (3)$$

2.2. Turbulence Model

Turbulent mixing overwhelms molecular diffusion, which in turn controls the reaction rates. LOx/methane chemistry is infinitely fast and is dependent solely on turbulence mixing. Two equation SST k-ω model is used for turbulence closure, which employs k-ω model near solid walls and uses a blending function to convert it to k-ε formulation for free stream flow. The eddies are modelled using turbulent kinetic energy and kinetic energy specific dissipation. Equations for turbulent kinetic energy and turbulent dissipation are given below:

$$\frac{\partial}{\partial t}(\rho k) + u_l\frac{\partial}{\partial x_l}(\rho k) = R_{ij}\frac{\partial u_i}{\partial x_j} - C_\mu\rho\omega k + \frac{\partial}{\partial x_j}\left[(\mu + \mu_t\sigma_k)\frac{\partial k}{\partial x_j}\right] \quad (4)$$

Where R_{ij} is the turbulent stress tensor term, which is given by:

$$R_{ij} = \mu_t\left(\frac{\tilde{u}_i}{x_j} + \frac{\tilde{u}_j}{x_i}\right) - \frac{2}{3}\mu_t\frac{\tilde{u}_k}{x_k}\delta_{ij} - \frac{2}{3}\bar{\rho}k\delta_{ij}$$

$$\frac{\partial}{\partial t}(\rho\omega) + \mu_l\frac{\partial}{\partial x_l}(\rho\omega) = \frac{\gamma}{\nu_t}R_{ij}\frac{\partial u_i}{\partial x_j} - \beta\rho\omega^2 + \frac{\partial}{\partial x_j}\left[(\mu + \mu_t\sigma_\omega)\frac{\partial \omega}{\partial x_j}\right] + 2(1 - F_1)\rho\sigma_{\omega 2}\frac{1}{\omega}\frac{\partial k}{\partial x_j}\frac{\partial \omega}{\partial x_j} \quad (5)$$

Where F_1 is a blending function given as:

$$F_1 = tanh\left[\left(min\left(max\left(\frac{\sqrt{k}}{0.09\omega y}, \frac{500\nu}{y^2\omega}\right), \frac{4\rho\sigma_{\omega 2}k}{CD_{k\omega}y^2}\right)\right)^4\right] \quad (6)$$

And $CD_{k\omega}$ is a cross diffusion term given as:

$$CD_{k\omega} = max\left(2\rho\sigma_{\omega 2}\frac{1}{\omega}\frac{\partial k}{\partial x_j}\frac{\partial \omega}{\partial x_j}, 10^{-20}\right)$$

2.3. Equation of State (EOS)

The equation of state is used to determine thermodynamic as well as transport properties of propellants, which in turn affects the mixing and combustion process. Appropriate equation of state should be used to calculate properties of rocket engines propellants subjected to high pressure conditions, generally above critical points. Propellants show large variation in their thermodynamic properties close to critical points, which can't be modelled using Ideal gas equation. Literature reveals that real gas model is required to accurately predict the thermodynamic properties and corresponding characteristics. Various cubic equation of states are used for analyzing these thermodynamic properties. A general cubic equation of state is given as:

$$P = \frac{RT}{V - b + c} - \frac{a}{(V^2 + \delta V + \varepsilon)} \quad (7)$$

Where *P* is the absolute pressure, *R* is the ideal gas constant and *V* is the molar volume. In current study, real gas effects are taken into account using Soave-Redlich-Kwong cubic equation of state solved for molar specific volume. Term *a* represents the correction factor for intermolecular forces and *b* represents that of molecular size. δ is set to be equal to b, while c and ε are set to 0. Coefficients given in the equation are:

$$\alpha(T) = \alpha_0\left[1 + n\left(1 - \left({}^{T}/_{T_c}\right)^{0.5}\right)\right]^2$$

$$n = 0.48 + 1.574\omega - 0.176\omega^2$$

$$\alpha_0 = \frac{0.4274R^2T_c^2}{P_c}$$

$$b = \frac{0.08664RT_c}{P_c}$$

2.4. Combustion Model

Vigorous reactions occur in the combustion chamber operating at supercritical conditions. Lox-hydrogen/methane chemistry is infinitely fast and turbulent mixing dominates. In order to predict the flame shape and corresponding characteristics, turbulence based non-premixed probability density function (PDF) with chemical equilibrium approach is used. Combustion is simplified to mixing and mixture fraction approach is used to predict the flame characteristics related to combustion. Mixture fraction is a conserved scalar quantity, and the species concentrations are derived from predicted mixture fraction fields. The mass fraction, temperature and density parameters of the species can be related to mixture fraction along with the assumption of equal diffusivities of species.

For a two feed system, mixture fraction is given by

$$f = \frac{Z_i - Z_{i,ox}}{Z_{i,fuel} - Z_{i,ox}} \quad (8)$$

$Z_{i,fuel}$ and $Z_{i,ox}$ represents fuel inlet and oxidizer inlet species mass fractions. Since the mixture fraction is a conserved scalar quantity, its governing equation consists of no source term. The value of f varies from 0 in oxidizer stream to 1 in fuel stream. The transport equation for the mixture fraction can be simplified as

$$\frac{\partial}{\partial t}(\rho\bar{f}) + \nabla.(\rho\vec{v}\bar{f}) = \nabla.\left(\frac{\mu_t}{\sigma_t}\nabla\bar{f}\right) \quad (9)$$

2.5. Chemical Equilibrium

Chemical equilibrium approach is used for analysing the flame shape and corresponding thermodynamic characteristics. In this approach, the chemistry is assumed to be rapid enough for chemical equilibrium to always exist in molecular level. It can predict the formation of intermediate species and does not require knowledge of detailed chemical kinetics. The thermodynamic properties like temperature, density, mass fraction etc. are taken as functions of mixture fraction and can be calculated as

$$\emptyset_i = \emptyset_i(f) \quad (10)$$

2.6. Probability Density Function

An assumed shape probability density function is used to calculate average values for fluctuating scalars. The shape of the PDF function depends on the nature of turbulent fluctuations. The PDF shape is computed by the prediction of mean and variance of the scalars at each point in the flow field. The mean scalars can be related to instantaneous scalars as

$$\bar{\emptyset}_\iota = \int_0^1 P(f)\,\emptyset_i(f)df \quad (10)$$

P(f) denotes the probability density function. The turbulence chemistry interaction is accounted by using transport equation for mixture fraction variance which is given as:

$$\frac{\partial}{\partial t}(\rho\overline{f'^2}) + \nabla.(\rho\vec{v}\overline{f'^2}) = \nabla.\left(\frac{\mu_t}{\sigma_t}\nabla\overline{f'^2}\right) + C_g\mu_t(\nabla\bar{f})^2 - C_d\rho\frac{\varepsilon}{k}\overline{f'^2} \quad (11)$$

Where C_g and C_d are constants.

3. Computational domain and boundary conditions

A typical rocket engine consists of multiple injector elements, combustion chamber, converging diverging portion and a throat. Figure 2 displays Lox-hydrogen propulsion systems with multiple swirl coaxial injector elements placed at inlet. The existing Lox-hydrogen engine consists of 61 swirl injector elements and 48 cooling orifices placed in outermost row for cooling the chamber walls. The full three dimensional geometry is shown in Fig.2. It consists of 61 swirl coaxial injectors along with 48 film cooling elements in the outermost region on the face of the domain.

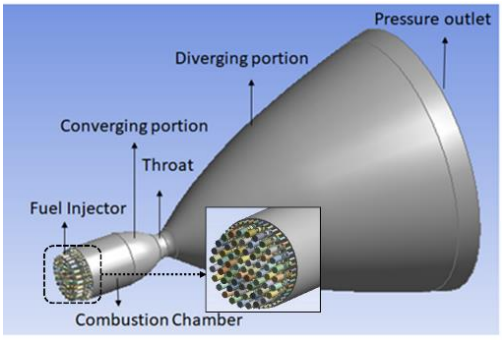

Figure 2 Full three dimensional domain

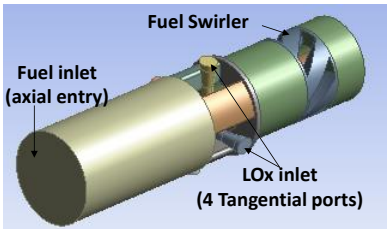

Figure 3 Single Element Configuration

Figure 3 shows schematic of single element with four tangential inlets for Lox entry and one axial inlet for fuel. A swirl has been imparted to LOx via tangential entry, whereas an opposite swirling action has been given to fuel with a 6 helical vane swirler placed in the fuel flow path.

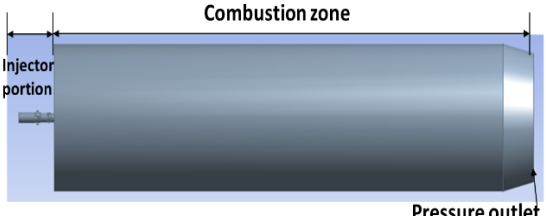

Figure 4 Computational domain

Figure 4 displays the computational domain used to analyze the combustion and flow characteristics. Domain with single element injector and combustion chamber is considered for analysis. An extended combustion zone of 790mm length and 200mm diameter is generated to capture flow features outside the injector element. LOx is introduced through four tangential inlets at 85K and methane/hydrogen through the axial inlet at 760/710K respectively. Mass flow boundary condition is applied at injector inlets and the outlet is given as pressure outlet. No slip and adiabatic boundary condition is imposed at the injector walls. Table 1 displays the operating conditions for both hydrogen and methane simulation cases.

Table 1 Operating conditions for single injector element

Engine Parameters	LOx/H_2	LOx/CH_4
Chamber Pressure (MPa)	6.8	6.8
LOx mass flow rate (kg/s)	0.246	0.306
Fuel mass flow rate (kg/s)	0.0405	0.087
LOx injection temperature (K)	85	85
Fuel injection temperature	710	760
Mixture Ratio	6.1	3.5

4. Validation study

A validation study is performed prior to simulation in single injector element to analyse the applicability of the chosen methodology. Computation is done in accordance with the domain and boundary conditions used by Kim et al. [14]. Figure 5 shows the computational domain and boundary conditions used in RCM-3(V04) test case. The flame shape and contours obtained were compared with the results from Kim et al. [14]. SRK equation of state has been used for simulation and a two equation RANS based, SST k-ω model is used for turbulence closure. Figures 6(a) and 6(b) shows the comparison of temperature contours from simulation and Literature. Validation study showed good agreement with literature results, with similar global flame shape and length. The role of kinetic mechanism used for flamelet generation in literature study can be the reason for differences in temperature contours. The overall reasonable comparison of flow features in literature and validation study shows the suitability of numerical methodology, which can be employed for further simulations.

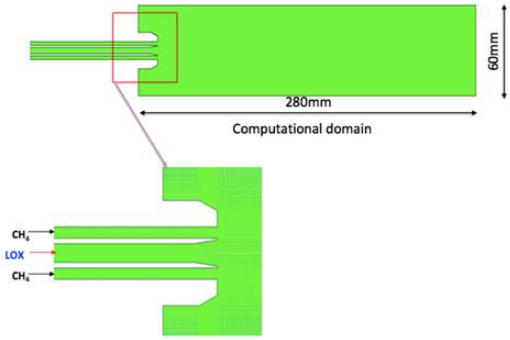

Figure 5 2D geometry for validation study

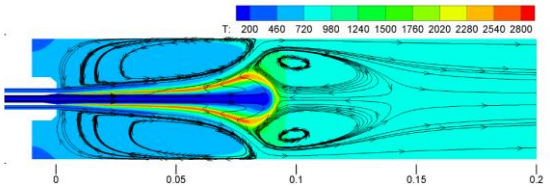

Figure 6(a) Temperature contour from Literature

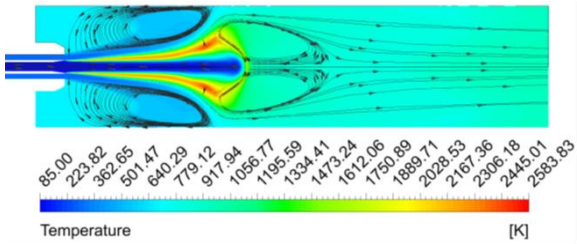

Figure 6(b) Temperature contour-Validation Study

5. Results and Discussion

A parametric three dimensional CFD study is conducted on single element swirl coaxial injector for LOx/hydrogen and LOx/methane propellant combination. A comparative study has been done to determine flow and flame dynamic characteristics for both hydrogen and methane. In order to understand differences in flow characteristics, a detailed cold flow simulation was done prior to combustion simulations.

5.1. Cold Flow Simulation Results

Cold flow simulation with solution of species equation is done to understand the

characteristic differences in flow field for hydrogen and methane in same injector.

5.1.1 Oxygen Mass Fraction Contours

Figure 7(a) shows the oxygen mass fraction contour at center cut plane for LOx/hydrogen case and Figure 7(b) for LOx/methane case. A substantial difference in the LOx core length is seen in two contour plots. An extended LOx core length is seen in the hydrogen case along with larger radial expansion compared to methane case.

The difference in Lox flow pattern is attributed to the low density of hydrogen which promotes larger expansion, both in radial and tangential directions. The combined effect of larger swirl velocity and radial expansion results in larger LOx core length in hydrogen case, whereas in Lox-methane simulation case, dense methane restricts the Lox flow both in radial and axial directions.

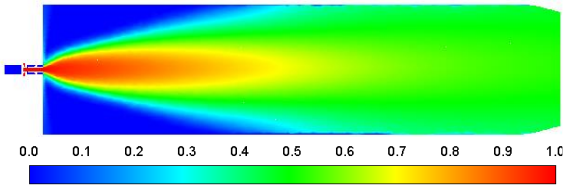

Figure 7(a) LOX mass fraction contour of LOx/hydrogen case

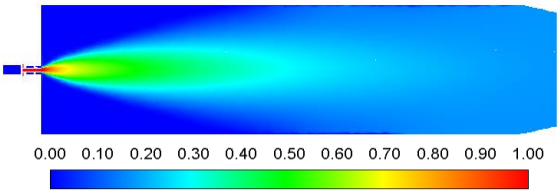

Figure 7(b) LOX mass fraction contour of LOx/methane case

5.1.2 Fuel Mass Fraction Contours

Figure 8(a) shows the hydrogen methane mass fraction contour and 8(b) shows the mass fraction contour for methane at center plane of computational domain.

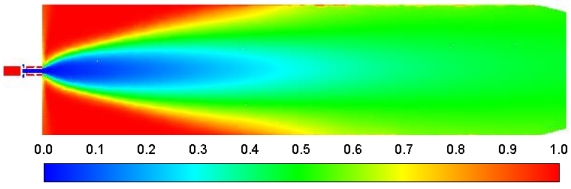

Figure 8(a) Hydrogen mass fraction contour

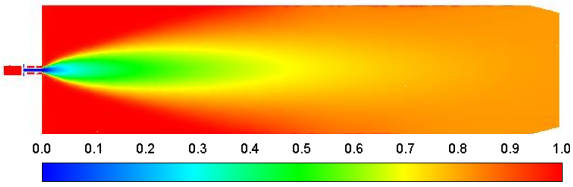

Figure 8(b) Methane mass fraction contour

It was also evident from methane mass fraction contour, that the radial expansion of LOx core is low in methane case compared to hydrogen case. The high temperature and low swirl velocity properties of methane do not allow the inner oxygen core to expand in radial direction in comparison to hydrogen case.

5.1.3 Density Trends

SRK real gas equation of state is used to predict the thermodynamic properties of the injected propellants. The contours shows accurate density prediction using SRK real gas model, with LOX density of 1183kg/m^3 calculated at inlet. Figure 9 shows close up view of the density trend observed near to the injected region in both methane and hydrogen cases. A rapid density reduction of LOx core is seen for both cases. Figure 10 shows the variation of density along the axial direction for both hydrogen and methane simulations.

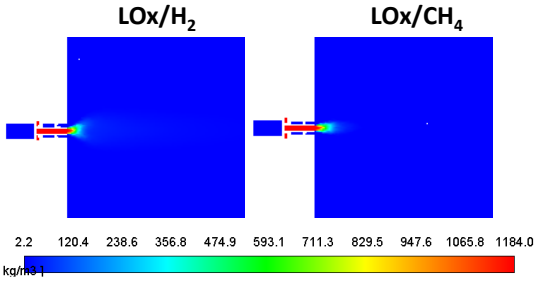

Figure 9 Density contour of LOx/hydrogen case

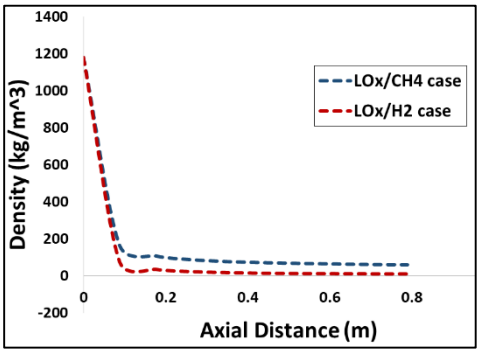

Figure 10 Density vs Axial Distance along the centre line for hydrogen and methane cases

5.1.4 Flow Characteristics

Swirl velocity characteristics in LOx/methane and LOx/hydrogen cases at axial distance from the injector head are analyzed to

understand the pattern observed for species mass fraction.

The low operating density of hydrogen can result in high swirl velocity which is also observed in Fig.11. It displays that, at same axial location swirl velocity in hydrogen case is much larger than methane case. This results in larger radial and tangential velocity components and more expansion of LOx core in LOx/hydrogen case.

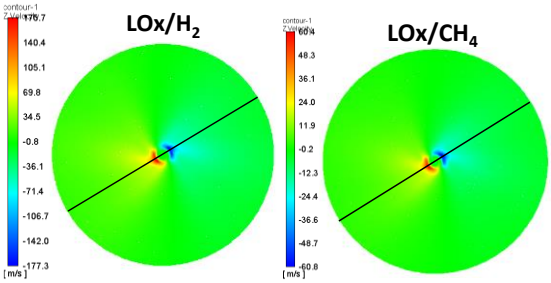

Figure 11 Swirl velocity contour at an axial location of 2mm from the injector for LOx/hydrogen and LOx/methane case

Figure 12 displays the swirl velocity plotted on line highlighted in Fig.11. The graph clearly shows the comparison of swirl velocity for both LOx/hydrogen LOx/methane propellant cases. It shows lower swirl velocity for methane case in comparison to hydrogen. The larger swirl velocity in hydrogen case is attributed to low density of hydrogen at injected conditions.

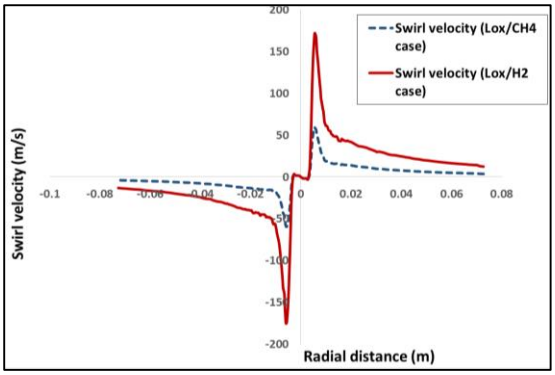

Figure 12 Swirl velocity vs Radial Distance at an axial location of 2mm from the injector post

5.2. *Combustion Results*

Detailed Combustion modelling is done on single element swirl coaxial injector with LOx/methane and LOx/hydrogen propellants to analyse the flame characteristics.

Validated numerical methodology based on Soave-Redlich Kwong(SRK) real gas equation of state, non-premixed combustion model with chemical equilibrium approach for chemistry closure and turbulence/chemistry interactions using assumed shape PDF approach is employed to model supercritical combustion.

5.2.1 *Flame Shape & Temperature Distribution*

Flame shape & structure for hydrogen and methane is analyzed from static temperature plot at cut plane. Figure 13 & 14 shows the static temperature contour of both LOx/hydrogen and LOx/methane propellant cases respectively. Both static temperature contours display the formation of high temperature zone/coaxial jet flame in shear layer between LOx jet and methane/hydrogen jet. The flame develops in the shear layer formed by mixing of propellants in the wake of LOx post. Both contours show flame to anchor/stabilize close to the surface of LOx post, whereas most part of combustion occurs in the proximity region of shear layer.

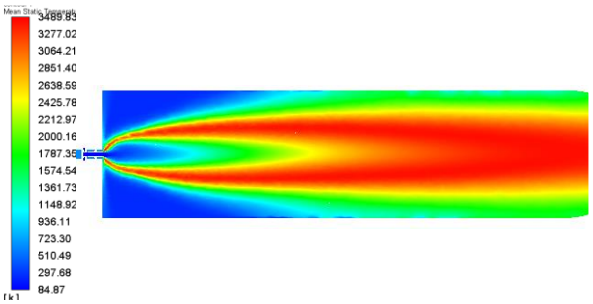

Figure 13 Temperature contours of hot gas in LOx/hydrogen case

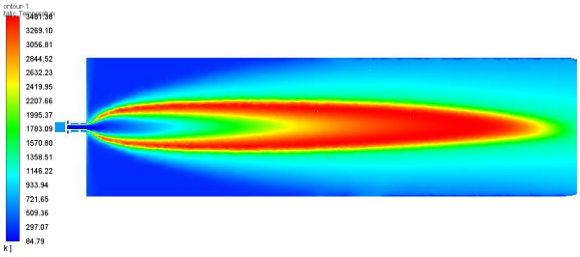

Figure 14 Temperature contours of hot gas in LOx/methane case

A substantial difference in flame expansion is observed between hydrogen and methane cases. A larger radial expansion of high temperature zone in hydrogen case, as attributed to low density and high swirl velocity of incoming hydrogen is captured, Figure 14 shows lesser radial expansion of high temperature zone, which is due to entrainment of high density methane from the top surface. A restrained flame expansion in radial and tangential direction is seen in comparison to hydrogen case.

Due to high swirl velocity in LOx/hydrogen case, shear layer diffusion is reduced, which eventually resulted in delayed mixing and high temperature combustion zone extending up to the exit of computational domain. In LOx/methane case, due to restrained radial expansion and higher diffusion, LOx core is consumed and high temperature combustion zone ends with in the domain.

Both cases showed flame to anchor at LOx post along with formation of recirculation zone which acts as a source of heat energy and aids in flame stabilization and igniting the incoming propellants.

Figure 15 shows the variation of temperature along the centreline for both propellant combinations. It displays linear increase in temperature from injector outlet to the point of ignition. A decrease in temperature for LOx/methane case is seen, whereas high swirl velocity in LOx/hydrogen case has results in delayed combustion and prolonged flame structure as displayed in temperature contours.

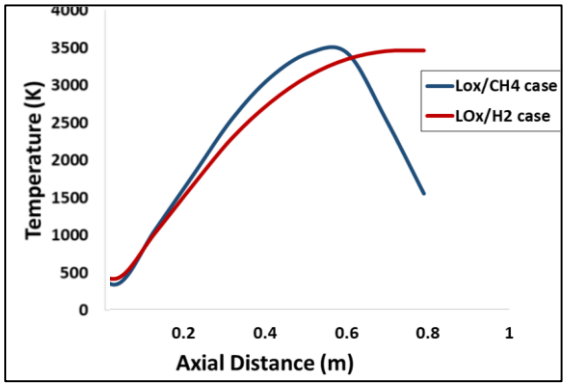

Figure 15 Temperature (K) variation along the axial direction for LOx/methane and LOx/hydrogen cases

5.2.2 *Hot Flow Characteristics*

Flow characteristics were compared for both hydrogen and methane combustion cases. Fig.16. displays swirl velocity pattern for both at a circular plane 2mm away from injector outlet.

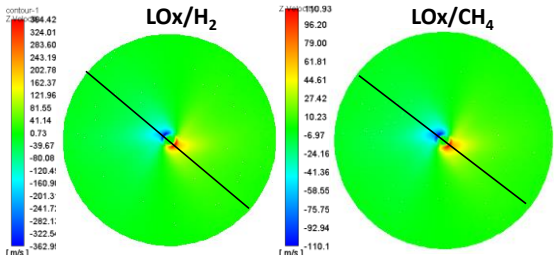

Figure 16 Swirl velocity (m/s) contour at an axial location of 2mm from the injector for LOx/hydrogen & LOx/methane cases

Swirl velocity in combustion simulations also showed similar trend as observed in cold flow. A large swirl velocity is seen in hydrogen case in comparison to methane. A comparatively high density of methane results in low swirl velocity, which has led to better mixing through the shear layer and effective combustion with in the domain, as seen above.

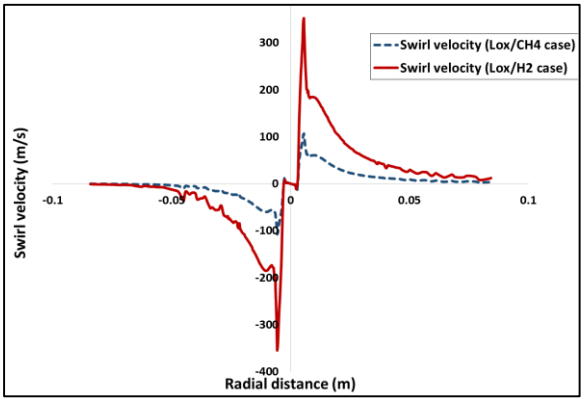

Figure 17 Swirl velocity vs Radial Distance at an axial location of 2mm from the injector post

Figure 17 shows the variation of swirl velocity in the radial direction over the line highlighted in Fig.16. The swirl velocity in LOx/hydrogen case is 364 m/s, while at the same location, the swirl velocity for LOx/methane combination is 110 m/s. This large difference in swirl velocity owes only to density difference between hydrogen and methane and has eventually effected the flame expansion pattern.

5.2.3 *Oxygen mass fraction contours*

The pseudo-boiling phenomenon plays a major part in controlling the LOx flow as it introduced at transcritical conditions (85K). Pseudo-boiling effect causes a change in behaviour of the injected propellant, unlike that in supercritical conditions. In this condition most of the energy absorbed from the hot gas will be used for volume expansion rather than increase in temperature. Figure 18 shows the LOx mass fraction contours of LOx/hydrogen LOx/methane cases. LOx mass fraction contour also shows enhanced radial expansion of LOx in hydrogen case than methane, which can be attributed to combined effect of higher swirl velocity and rapid volume expansion.

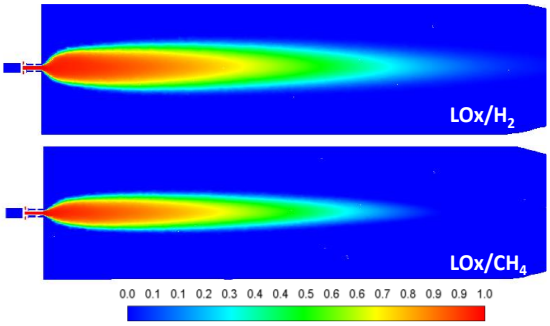

Figure 19 Oxygen mass fraction contour in LOx/hydrogen case

5.2.2 Fuel mass fraction contours

In similar way fuel mass fraction in combustion simulations is also compared to understand the hydrogen/methane flow through same injector element. Figure 20 shows the fuel mass fraction contours of LOx/methane and LOx/hydrogen cases respectively.

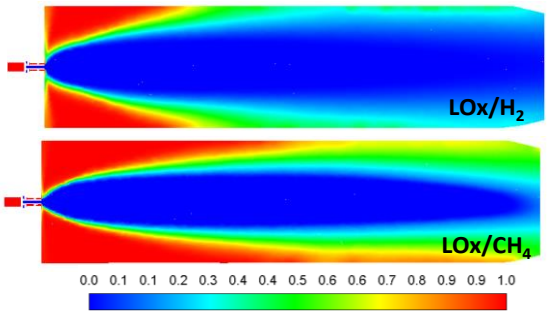

Figure 20 Hydrogen mass fraction contour

The combined effect of higher temperature (760 K) and low swirl velocity in the LOx/methane case do not allow the inner oxygen core to expand in radial direction, in comparison to LOx/hydrogen case. The larger swirl velocity, owing to the low density property of hydrogen, allows the LOx core to expand in radial and tangential direction, and further affects the shear layer diffusion.

The combustion simulation illustrated the characteristic difference of operating LOx-methane in swirl coaxial injector of hydrogen propulsion system. The restricted flame expansion for methane case is only attributed to modified thermophysical properties of operating fuel.

6 Conclusion

A systematic investigation of LOx-methane combustion in single element injector of existing hydrogen propulsion system has been conducted numerically at supercritical conditions. Numerical methodology with non-premixed chemical equilibrium model with assumed PDF approach is used for analysing the combustion phenomenon in three-dimensional domain. A validated numerical methodology was developed using Mascotte Chamber RCM-3(V04) test case results. Cold flow characteristics were studied to understand the flow filed pattern prior to combustion simulations. Combustion characteristics of both hydrogen and methane are analysed at chamber pressure of 6.8MPa. A detailed comparison of hydrogen and methane flame shape in single element domain is carried out. Results showed that both methane and hydrogen combustion displayed similar flame characteristics, with flame initiating from LOx post and developing in shear layer. A larger and rapid radial expansion of flame was seen for hydrogen compared to LOX-methane case, which is attributed to different thermophysical properties at injection conditions. Both simulations showed, flame anchored at fuel post and formation of recirculation region to help in flame stabilization by further igniting the incoming propellants.

The current study highlighted the combustion characteristics of LOx/methane in injector element of existing hydrogen propulsion system. It highlighted the usability of same injector configuration for possible conversion of LOx-hydrogen engine. The current study indicated better mixing and confined combustion for LOx/methane operation. The current methodology is successfully implemented at single element level and can be extended to multi injector domain in future.

7 References

[1] Wolfgang O.H. Mayer, and Joshua J. Smith. Fundamentals of supercritical mixing and combustion of cryogenic propellants. AIAA, 2004.

[2] Congiunti, C. Bruno, and E. Giacomazzi,Supercritical Combustion Properties, in:AIAA Paper 2003-0478, 2003.

[3] Emre Sozer, Aravind Vaidyanathan, Corin Segal, and Wei Shyy, Computational Assessment of Gaseous Reacting Flows in Single Element Injector, AIAA, 2009.

[4] Strakey P.A, D. G. Talley, and J. J. Hutt, Mixing Characteristics of Coaxial Injectors at High Gas/Liquid Momentum Ratios, J. Propul. Power, 2001.

[5] Liang Li, Maozhao Xie, Wu Wei, Ming Jia, and Hongsheng Liu. Numerical investigation on cryogenic liquid jet under transcritical and supercritical conditions. Cryogenics, 16-128.

[6] Shingo Matsuyama et al. Large Eddy Simulation of CH_4/O_2 Combustion of a Swirl Coaxial Injector, AIAA, 2014.

[7] Ata Poormahmood, Mohammad Shahsavari, and Mohammad Farshchi. Numerical

investigation of cryogenic swirl inection under supercritical conditions. Journal of Propulsion and Power, Vol 34, No: 2.

[8] Takao Inamura, Hiroshi Tamura, Hiroshi Sakamoto. Characteristics of Liquid Film and Spray Injected from Swirl Coaxial Injector. Journal of Propulsion and Power, Vol 19, No:4. 2003.

[9] Baoe Yang, Francesco Cuoco, and Michael Oschwald, Atomization and Flames in LOX/H_2 and LOX/CH_4 Spray Combustion, J. Propul. Power, 23, 2007.

[10] Dalphin Salgues, Ann-Geraldine Mouis, Seong-Young Lee, Danielle Kalitan, Sibtosh Pal and Robert Santoro, Shear and Swirl Coaxial Injector Studies of LOX/GCH_4 Rocket Combustion Using Non-Intrusive Laser Diagnostics, AIAA, 2006.

[11] Vigor Yang, and Xingjian Wang. Supercritical Mixing and Combustion of Liquid-Oxygen/Kerosene Bi-Swirl Injectors, J. Propul. Power, 2006.

[12] Huo .H and V. Yang, Large Eddy Simulation of Supercritical Combustion of Liquid Oxygen and Kerosene of a bi-Swirl Coaxial Injector,in:AIAA Paper 2013-0429, 2013.

[13] Cutrone .L, Battista, and Ranuzzi. Supercritical high pressure combustion simulation for LOx/CH_4 rocket propulsion systems. AIAA, 2008.

[14] Taehoon Kim, Yongmo Kim, and Seong-Ku Kim. Effects of pressure and inlet temperature on coaxial gaseous methane/liquid oxygen turbulent jet flame under trans-critical conditions. The Journal of Supercritical Fluids, 81:164, 174, 2013.

[15] Liang Li, Maozhao Xie, Wu Wei, Ming Jia, and Hongsheng Liu. Numerical investigation on cryogenic liquid jet under transcritical and supercritical conditions. Cryogenics, 16-128.

[16] Mayer .W, A. Schik, and M. Schaffler. Injection and mixing in high pressure liquid oxygen/gaseous hydrogen rocket combustors. J. of Supercritical Fluids, 2000.

[17] Hickey .J .P, and M. Ihme. Supercritical mixing and combustion in rocket propulsion. Centre for Turbulence Research, Annual Research Brifs, 2013.

[18] Singla G, Scouaire P. Rolon C.C.S, Zurbach S, and Thomas J. Experiments and simulations of LOx/CH_4 combustion at high pressures. Proc. Combust. Inst, 30:2921 {2928, 2005}.